Long-Term Improvement of Parkinson Disease Motor Symptoms Derived From Lesions of Prelemniscal Fiber Tract Components

Maria Guadalupe García-Gomar, MD, PhD*
Luis Concha, MD, PhD*
Julian Soto-Abraham, MD, MSc‡
Jacques D. Tournier, MD§ ¶
Gustavo Aguado-Carrillo, MD, MSc‡
Francisco Velasco-Campos, MD‡

*Institute of Neurobiology, Universidad Nacional Autónoma de México, Campus Juriquilla, Juriquilla, Mexico; ‡Unit for Stereotactic and Functional Neurosurgery, General Hospital of Mexico, Ciudad de México, Mexico; §Department of Biomedical Engineering, School of Bioengineering and Imaging Sciences, King's College London, King's Health Partners, St. Thomas' Hospital, London, United Kingdom; ¶Centre for the Developing Brain, School of Bioengineering and Imaging Sciences, King's College London, King's Health Partners, St. Thomas' Hospital, London, United Kingdom

Correspondence:
Francisco Velasco Campos, MD,
Unit for Stereotactic and Functional Neurosurgery,
General Hospital of Mexico,
Dr Balmis 148,
Col Doctores,
Del Cuauhtémoc,
Ciudad de México, CP 06720, Mexico.
Email: slanfe@prodigy.net.mx

Received, March 10, 2019.
Accepted, April 15, 2020.

BACKGROUND: Prelemniscal radiations (Raprl) are composed of different fiber tracts, connecting the brain stem and cerebellum with basal ganglia and cerebral cortex. In Parkinson disease (PD), lesions in Raprl induce improvement of tremor, rigidity, and bradykinesia in some patients, while others show improvement of only 1 or 2 symptoms, suggesting different fiber tracts mediate different symptoms.

OBJECTIVE: To search for correlations between improvements of specific symptoms with surgical lesions of specific fiber tract components of Raprl in patients with PD.

METHODS: A total of 10 patients were treated with unilateral radiofrequency lesions directed to Raprl. The improvement for tremor, rigidity, bradykinesia, posture, and gait was evaluated at 24 to 33 mo after operation through the Unified Parkinson's Disease Rating Scale (UPDRS) score, and the precise location and extension of lesions through structural magnetic resonance imaging and probabilistic tractography at 6 to 8 mo postsurgery. Correlation between percentage of fiber tract involvement and percentage of UPDRS-III score improvement was evaluated through Spearman's correlation coefficient.

RESULTS: Group average improvement was 86% for tremor, 62% for rigidity, 56% for bradykinesia, and 45% for gait and posture. Improvement in global UPDRS score correlated with extent of lesions in fibers connecting with contralateral cerebellar cortex and improvement of posture and gait with fibers connecting with contralateral deep cerebellar nuclei. Lesion of fibers connecting the globus pallidum with pedunculopontine nucleus induced improvement of gait and posture over other symptoms.

CONCLUSION: Partial lesion of Raprl fibers resulted in symptom improvement at 2-yr follow-up. Lesions of selective fiber components may result in selective improvement of specific symptoms.

KEY WORDS: Correlation of fiber tracts lesions and improvement of symptoms, DWI-MRI, Parkinson disease, Prelemniscal radiations, Probabilistic tractography, Radiofrequency lesions, Tract density image

Operative Neurosurgery 0:1–12, 2020 DOI: 10.1093/ons/opaa186

Spiegel and Wycis[1] first proposed the term "campotomy" to suggest that subthalamic fibers could represent more discrete targets to treat motor symptoms of Parkinson disease (PD), as compared with the conventional pallidal and thalamic lesions. The observation made by Andy and Jurko[2] that the simple insertion of an electrode 2.0 mm in diameter

ABBREVIATIONS: 3D, 3-dimensional; **AC-PC,** anterior commissure-posterior commissure; **CCx,** contralateral cerebellar cortex; **CSD,** constrained spherical deconvolution; **DBS,** deep brain stimulation; **DCN,** deep cerebellar nuclei; **DWI-MRI,** diffusion-weighted magnetic resonance imaging; **FLAIR,** Fluid attenuated inversion recovery; **FSL,** FMRIB software library; **GP,** globus pallidum; **GP-PPN,** globus pallidum-peduncle pontine nucleus; **L-DOPA,** l-deoxy phenylalanine; **MES,** mesencephalic tegmentum; **MRI,** magnetic resonance imaging; **OFC,** orbitofrontal cortex; **PD,** Parkinson disease; **PFC,** prefrontal cortex; **PPN,** peduncle pontine nucleus; **PSA,** posterior subthalamic area; **Pu,** putamen; **Raprl,** prelemniscal radiations; **RF,** radiofrequency; **Ru,** red nucleus; **SD,** standard deviation; **SIFT2,** spherical-deconvolution informed filtering of tractograms; **STN,** subthalamic nucleus; **S-W,** Schaltenbrand-Wahren; **TDI,** track-density image; **UPDRS,** Unified Parkinson's Disease Rating Scale

TABLE 1. Demographics of Population

Patients	Sex	Age (years)	Years of evolution	Operated side	Follow-up months
P01	F	51	5	Left	31
P02	F	52	5	Right	33
P03	M	71	3	Right	30
P04	M	53	5	Left	32
P05	F	52	8	Left	32
P06	F	58	2	Right	31
P07	M	66	8	Left	24
P08	M	72	11	Left	30
P09	M	74	14	Left	29
P10	M	55	5	Left	30
Global	M = 6	60.4 (8.84)	6.36 (3.58)	Left = 7 (70%)	32.90 (9.28)
(Mean and standard deviation [SD])	F = 4			Right = 3 (30%)	

M = male, F = female.

in the posterior subthalamic area (PSA) induced a complete arrest of tremor in the contralateral side made a proof of principle of the original proposal. Subsequent reports identified the target as a group of fibers in the PSA named prelemniscal radiations (Raprl).[3-6] When deep brain stimulation (DBS) became available, Raprl-DBS was found also effective in treating rigidity, bradykinesia, posture, and gait.[7,8]

Raprl is composed of different fiber tracts, connecting the brain stem and cerebellum with the basal ganglia and cerebral cortex, as demonstrated by high angular resolution diffusion-weighted magnetic resonance imaging (DWI-MRI) and tractography, which identified 3 fiber components: cerebellar-thalamic-cortical, globus pallidum-peduncle pontine nucleus (GP-PPN), and mesencephalic-orbitofrontal component.[9] Lesions[2-6] or DBS[7,8,10-12] of Raprl can induce improvement of tremor, rigidity, bradykinesia, posture, and gait in some patients, while others show improvement of only 1 or 2 of those symptoms. The selective improvement of one symptom over the others suggests that different fibers might be related to different symptoms.[11,12]

On the other hand, even when DBS therapy has been considered the gold standard to treat motor symptoms of PD, lesions induced by radiofrequency (RF), radiosurgery, or magnetic resonance imaging (MRI)-guided ultrasound are still used to treat PD cases.[13-15] This applies to patients and health services that cannot afford the cost of neurostimulators, patients living in areas with no infrastructure to monitor DBS therapy and its complications, and cases with dominant unilateral symptoms.[16] We have taken the opportunity of treating a series of patients with dominant unilateral PD symptoms, performing discrete unilateral RF lesions. Since lesions are distinctly identified in structural MRI, we analyzed the site and extent of lesions and their spatial relation to tractography of the subthalamic region, correlating percentage involvement of specific fiber systems with percentage improvement of specific symptoms evaluated through the Unified Parkinson's Disease Rating Scale-III (UPDRS-III).

METHODS

The protocol was approved by the Hospital's Institutional Review Board/Ethics Committee, and every participant signed an informed consent, and fully complied with the declaration of Helsinki.

A total of 10 PD patients (ages 54-74 yr) with dominant unilateral symptoms were included in the study: 2 patients in stage I, 6 in stage II, and 2 in stage III of the Hoehn-Yahr scale. All patients improved by L-deoxy phenylalanine (L-DOPA) administration for 3 to 9 yr; thereafter, they presented motor fluctuations and/or L-DOPA-induced dyskinesias. A total of 7 patients had prominent symptoms on the right extremities and 3 on the left (Table 1). Severity of symptoms was evaluated through UPDRS-III motor score-specific items: 20 to 21 for tremor; 22 for rigidity; 23 to 26 and 31 for bradykinesia; and 27 to 30 for gait and posture. Pre- and postoperative evaluations were performed in a 24 h off-medication condition.

Surgery was carried out under local anesthesia, contralateral to more prominent symptoms. Electrode trajectory was planned through a fusion imaging of preoperative MRI and computed tomography scan in stereotactic conditions with the ZD frame (Leibinger, Freiburg, Germany) in place, using the Praezis Plus 3A software (Praezis, Heidelberg, Germany). T2 axial sequences oriented parallel to the inter-commissural (anterior commissure-posterior commissure [AC-PC]) line, 1-mm-thick sections without intervals, clearly identified the red nucleus (Ru) and subthalamic nucleus (STN) between 2 and 5 mm below AC-PC. The target was the white matter between anterior-lateral margin of Ru and the posterior medial margin of STN. The target was located at the level of the maximal diameter of Ru, usually 3 to 4 mm below the AC-PC line[12] (Figures 1-3).

Electrical stimulation was applied through a RF bipolar electrode 1.6 mm in diameter, with a center-to-center contact distance of 3.0 mm (thermo-controlled bipolar electrode TCB-013, Fischer Leibinger, Freiburg, Germany). Stimulation parameters were 60 Hz, 0.5 ms, and amplitude increased in steps of 0.5 V along the trajectory of the electrode, starting 4.0 mm above the target point in 2-mm steps. Usually, 4 steps were necessary to identify the optimum place for lesioning based on the amplitude of stimulation to control symptoms without side effects, although in some cases, exploration extended to 6 levels, as described for patients P05 and P08 in the discussion section. Lesions were performed at a temperature of 80°C for 60 s.

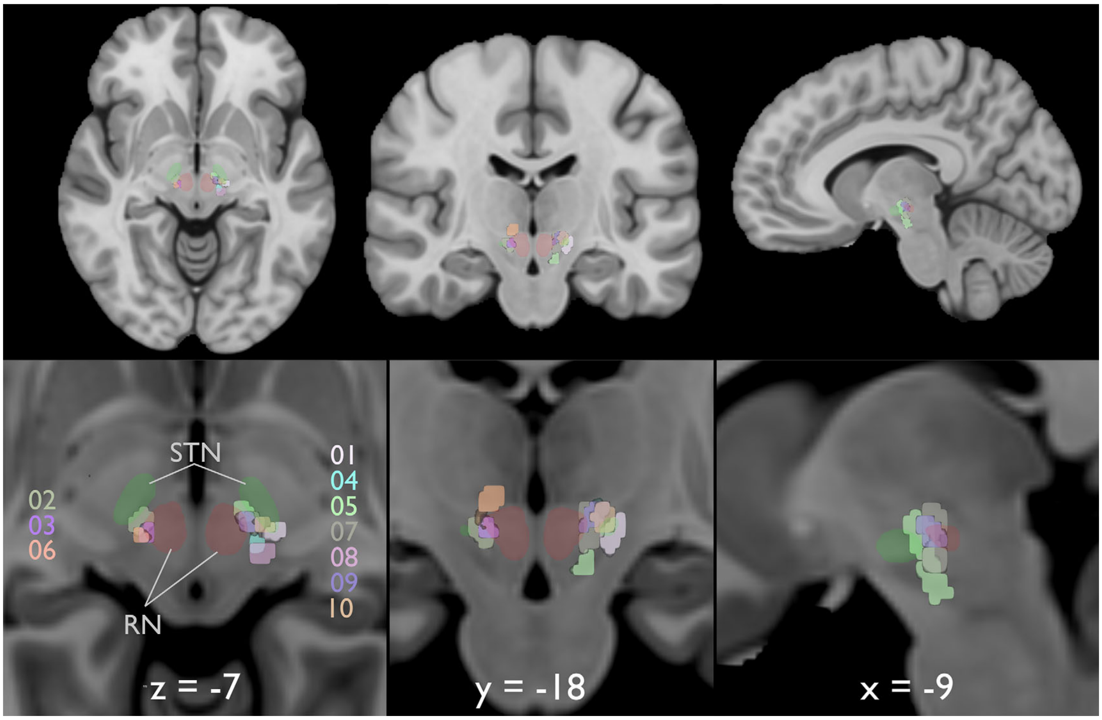

FIGURE 1. *Projection of individual lesions produced by RF ablation into standard space, color-coded by patient and organized by hemisphere. The majority of lesions involve white matter between STN and Ru, corresponding to the location of the prelemniscal radiations. Coordinates in mm. Notice that the target extends in the dorsal-ventral (Z) direction more than anterior-posterior (Y) and medial-lateral (X) coordinates.*

Final evaluation was through UPDRS-III applied 24 to 33 mo postoperatively, avoiding transient improvements.

Pre- and postoperative MRI were obtained using an identical protocol with a 3T Philips Achieva TX MRI scanner (Philips Medical Systems, Best, Netherlands). High-resolution T1-weighted (3-dimensional [3D]) gradient echo images were acquired with a spatial resolution of $1 \times 1 \times 1$ mm^3 (TR/TE = 8.05/3.68 ms) and sagittal plane 3D fluid attenuated inversion recovery; (FLAIRT2) sequences ($1 \times 1 \times 1.2$ mm^3 resolution; TR/TI/TE = 4800/1650/279 ms). DWI-MRI was acquired with 120 unique diffusion-gradient directions, with b = 2000 s/mm^2, voxel size of $2 \times 2 \times 2$ mm^3, and 4 non-DWI (b = 0 s/mm^2). The scanning session was 50 min. MRI follow-up was performed 6 to 8 mo postsurgery to eliminate the artifacts of an inflammatory process induced RF lesioning.

Diffusion Preprocessing and Tractography

DWIs were corrected for motion and eddy-current distortions using FMRIB software library (FSL). Images were intensity-normalized by dividing the diffusion-weighted volumes by the median value of cerebrospinal fluid intensity on the mean b = 0 image. Fiber orientation distributions were estimated using constrained spherical deconvolution (CSD)[17] with MRtrix3 (http://www.mrtrix.org/).

Tractography characterized tracts that traverse lesions. We analyzed the anatomical connectivity obtained in the preoperative tractography data, since diffusion changes induced by the lesions impact negatively the accurate delineation of the affected tracts on the postoperative DWI.[18] Postoperative anatomical MRI was used to manually delineate the ablation, which was registered to presurgical tractography, and assessed the involvement of the preoperative tracts within the coregistered lesion.

Registration of DWI to the anatomical T1-weighted image was performed using a linear transformation. Automatic cortical parcellation was performed on T1 images with FreeSurfer (v.5.3, http://surfer.nmr.mgh.harvard.edu).[19] For a detailed segmentation of the subcortical nuclei, VolBrain (http://VolBrain.upv.es) was used.[20] For each T1 volume, tissue maps (cerebrospinal fluid, gray and white matter) were obtained using FSL-FAST.

To improve visualization of the small anatomical structures within the PSA, track-density images (TDIs)[21] based on CSD[17] were generated from 10 000 000 tracts seeded throughout the white matter with a final resolution of $0.2 \times 0.2 \times 0.2$ mm^3. The ability of TDI to resolve sub-voxel structures has been demonstrated in synthetic as well as biological data.[21-24] TDI maps, along with co-registered FLAIRT2 volumes, were used to guide manual segmentation of the PSA aided by the Schaltenbrand-Wahren (S-W) atlas,[25] delineating the following structures: STN, Ru, and Zic.[9,26] Probabilistic tractography was performed using the anatomically constrained tractography method.[27] Uniform seeding across the entire white matter was used to generate 100 000 000 streamlines (tracts). To have a quantitative measurement of the tracts, we seeded an additional 1 000 000 streamlines in our region of interest (Raprl), combined them with the 10 000 000 whole-brain streamlines, and performed spherical-deconvolution informed filtering of

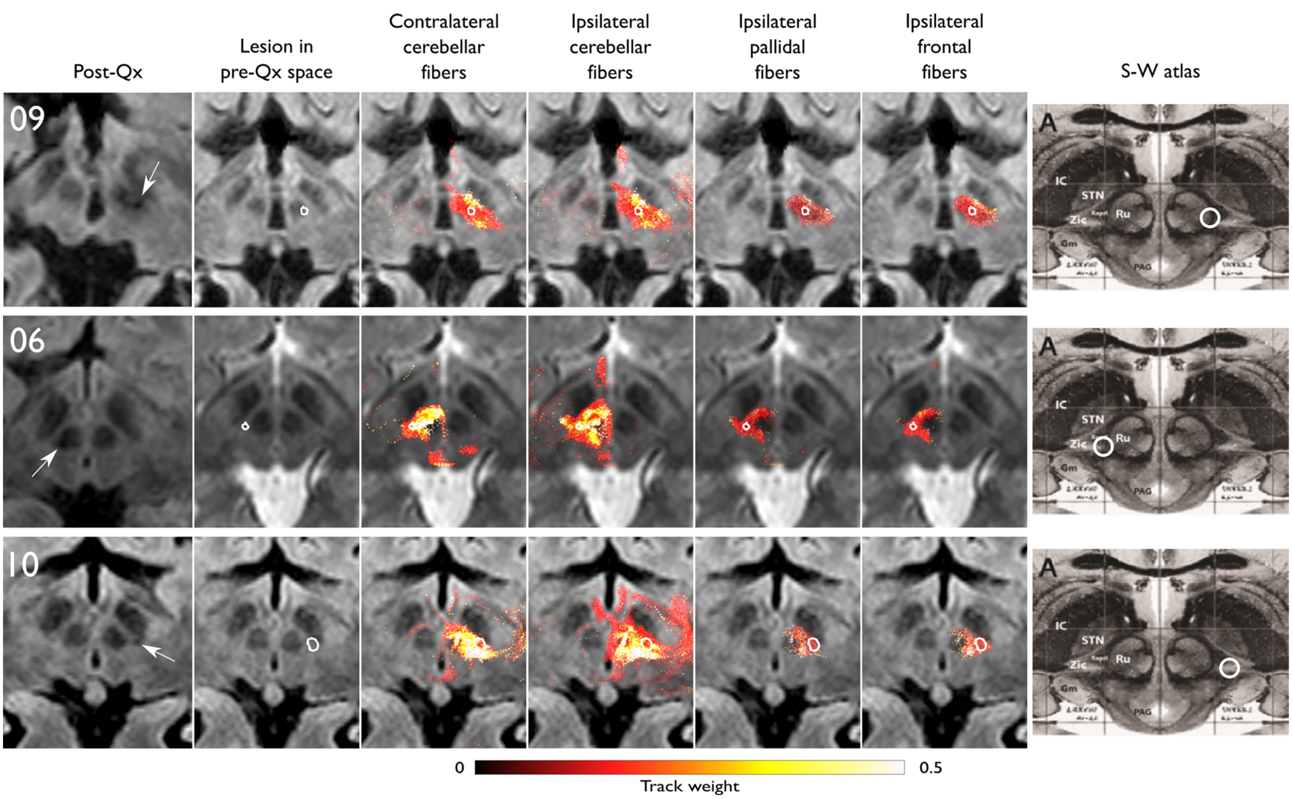

FIGURE 2. *Cases with homogeneous improvement of symptoms induced by lesions in Raprl. Columns from left to right show the following: postsurgical MRI (Post-Qx) with lesion locations indicated by arrows. Second column = lesions automatically superimposed on presurgical space. The following 4 columns show different fiber tracts in Raprl at the level of lesions, visualized as semitransparent streamlines. The last column shows lesions on the axial view of S-W stereotactic atlas 3.5 mm below the AC-PC level (Hv-3.5).*

tractograms (SIFT2) obtaining quantitative estimates of white matter density, given as the sum of SIFT2 weights for the streamlines in a given pathway.[28,29] "Tracts were virtually dissected according to cortical frontal areas, basal ganglia, and cerebellum, defined automatically by the co-registration of subject-specific labels according to the Desikan-Killiany Atlas."[19] The regions were grouped according to different greater anatomical areas, as explained in the results section.

The precise location and extension of the lesion was evaluated at 6 to 8 mo after surgery. Lesions were manually delineated using the FLAIRT2 postoperative volume, where the lesion was clearly distinguished, and were linearly registered to the postoperative TDI. In this way, we were able to determine the percentage of each tract involved by lesions.

Lesion involvement of each fiber tract represented the percentage of the sum of SIFT2 weights for the subset of streamlines that pass through the segmented lesion, relative to the sum of SIFT2 weights for all streamlines conforming the tracts.[30] To achieve their normalization, we concatenated the linear registration between each subject's postsurgical to presurgical volumes, and the nonlinear transformation of each subject's presurgical T2-weighted volume to standard space (ICBM-152 2009b, nonlinear asymmetric).[31]

Statistical Analysis

Symptom improvement is referred as the percentage decrease of UPDRS postoperative score with respect to preoperative values; all evaluations were performed in a 24-h off-medication condition. Changes from preoperative and final follow-up UPDRS scores and sub-scores for tremor, rigidity, bradykinesia, gait, and posture were determined and their significance evaluated by Wilcoxon's test.

The relationship between changes in percentage decrease in the score of items for different symptoms and percentage decrease in weight of tracts connecting to different frontal cortical and subcortical regions involved in lesions was determined through Spearman's correlation coefficient.

RESULTS

Volumes derived from segmentation of anatomical structures in PSA for Ru and STN were similar to those reported by other authors,[32,33] while volumes for Raprl and Zic were similar in both hemispheres of the same patient, indicating that the segmentation process was reliable. RF ablations were localized to regions identified as Raprl and Zic, according to the S-W atlas. Nonlinear

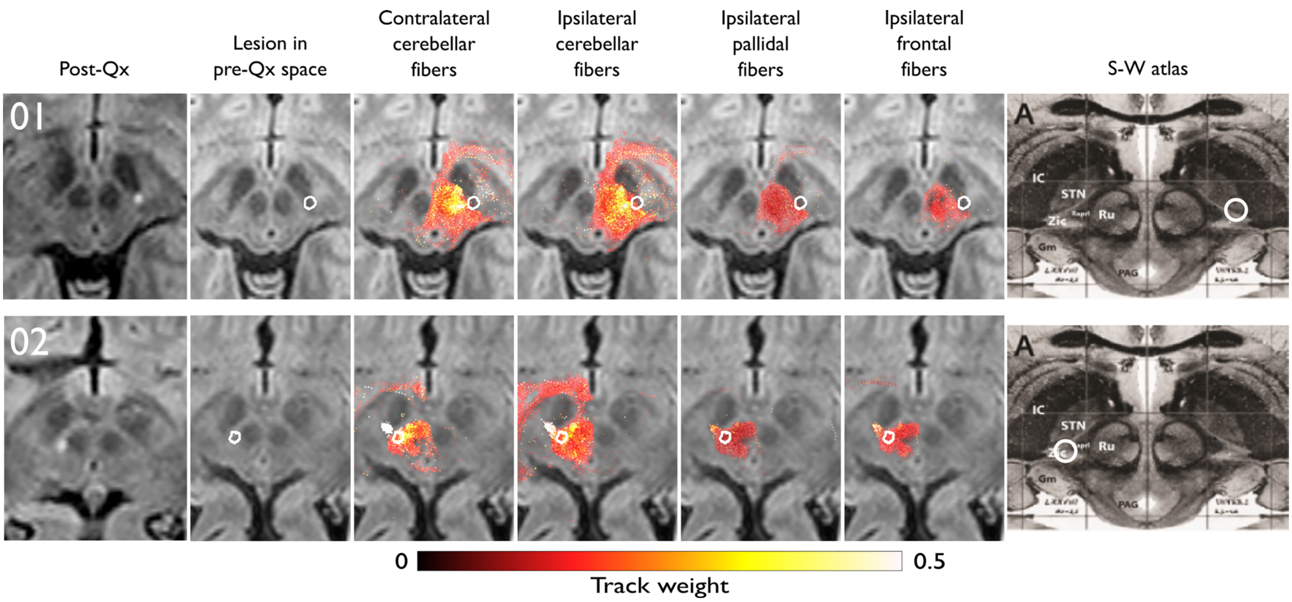

FIGURE 3. *Cases with transient improvement of symptoms; columns as for Figure 2. P01 (top) shows a lesion immediately behind the posterior pole of STN, corresponding to Zic. P02 (bottom) shows a lesion behind the maximal diameter of Ru, between Zic and medial lemniscus.*

registration of lesions showed the majority lying between Ru and STN (Figure 1). Examples of lesions in patient-specific images are shown in Figures 4 and 5.

Automated tractography analysis provided evidence of Raprl connectivity with 22 cortical-subcortical regions per hemisphere, which were combined into the following:

1. Bilateral orbitofrontal cortex (OFC): lateral and medial segments.
2. Prefrontal cortex (PFC): frontal pole, pars orbitalis, pars triangularis, and middle frontal gyrus.
3. Supplementary motor area including superior frontal gyrus.
4. Primary motor cortex.
5. Ipsilateral and contralateral cerebellar cortex (CCx) and deep cerebellar nuclei (DCN).
6. Globus pallidum (GP).
7. Caudal putamen (Pu).
8. Thalamus (Vop and Vim nuclei).
9. Ipsilateral and contralateral dorsal brainstem (peduncle pontine nucleus [PPN]).

The connectivity maintains somatotopic organization, showing an anterior-posterior disposition of streamlines reaching OFC, PFC (pars opercularis and ventral part of middle frontal gyrus), GP, Vop, Vim, PPN, CCx, and DCN, where fiber tracts that coalesce and funnel through Raprl are distinguishable mainly by their assigned SIFT2 weights.

Spearman correlation tests were positive for percentage lesion involvement for pathways connecting with contralateral CCx and clinical improvements assessed via contralateral UPDRS total score. UPDRS scores for gait and posture also showed a positive correlation with the percentage involvement of contralateral DCN with a larger proportion of streamlines included in the surgical lesions (Figure 5). In contrast, involvement of connectivity with dorsal-lateral PFC, Pu, and GP had a negative impact on gait and posture (Figure 6).

Preoperative/postoperative UPDRS-III evaluation demonstrated that tremor was the symptom best controlled by Raprl-RF lesioning in the studied group (86%, $P = .001$), followed by rigidity (62%, $P = .015$), bradykinesia (56%, $P = .046$), and gait and posture (45%, $P = .001$) (Table 2). At 2-yr follow-up, the mean value for UPDRS global score had decreased, although it did not reach statistical significance due to an increased score for symptoms in the nontreated extremities.

Improvement was considered optimum when reduction of the UPDRS-III score of items for one specific symptom was over 75%; patients considering symptom control very satisfactory in off-medication condition; suboptimum when symptoms decreased 50% to 75% and still required medication; and reduction of less than 50% off medication was considered a poor result.[11]

Individual improvements of symptoms for each patient and lesion size are displayed in Table 3, which also shows the progression of symptoms in the untreated side.

Six cases had optimum control of tremor, 2 cases had borderline suboptimum control (75% and 71.4%), and the other 2 cases had control of tremor immediately after surgery, lasting only 3 wk in 1 (P02) and 2 mo in the other (P01), and thereafter progressively reappeared, with reductions of 20% and 50% at 2-yr follow-up.

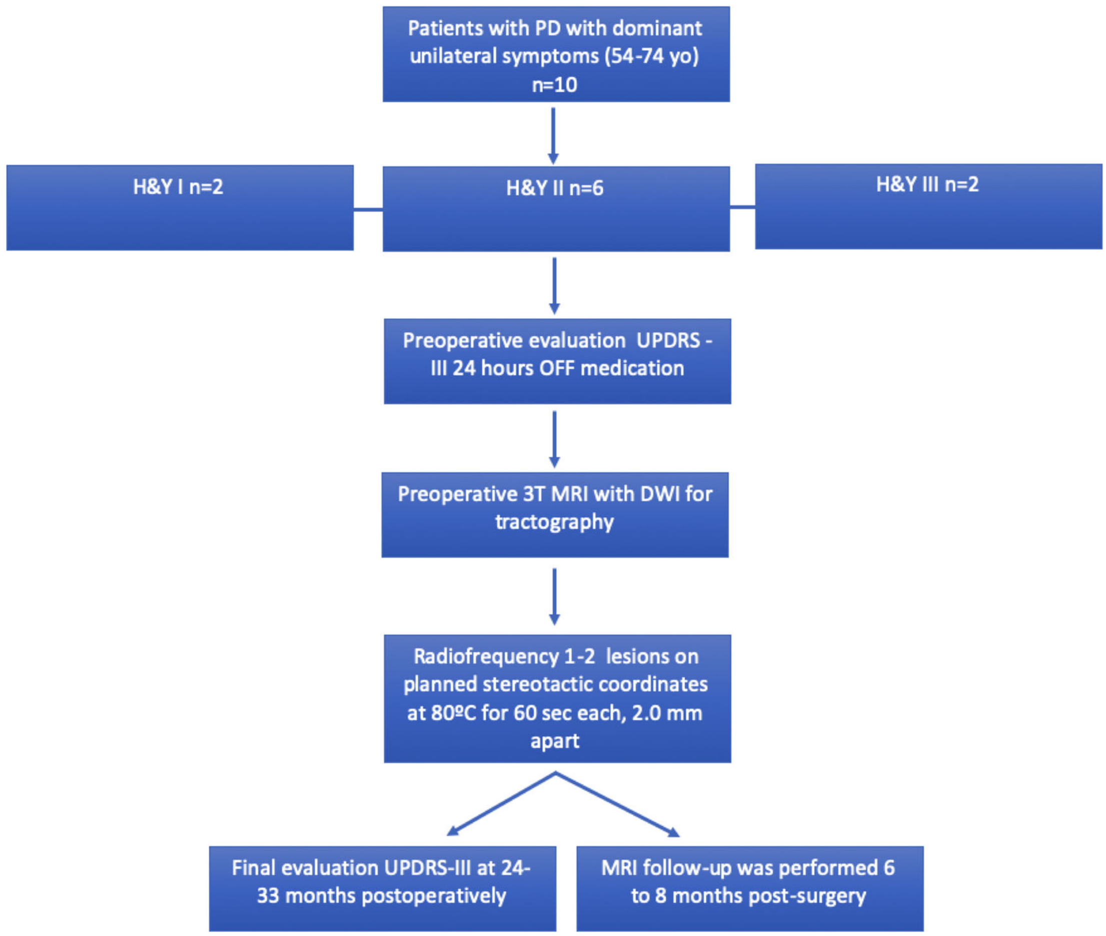

FIGURE 4. *Patient flowchart.*

In these cases, rigidity was unchanged in one and had increased 20% in the other, with poor control of bradykinesia, posture, and gait at the final evaluation. One case (P03) had optimum control of tremor with poor control of rigidity, bradykinesia, posture, and gait.

From 6 patients with optimum control of tremor, 4 had optimum control of rigidity, as well, and 2 had poor control (P03 and P05), while 1 case (P07) with suboptimum control of tremor had optimum control of rigidity.

Regarding bradykinesia, from 6 patients with optimum control of tremor, only 1 had optimum control of bradykinesia and 2 had suboptimum control.

From 6 cases with optimum control of tremor, 2 patients (P05 and P08) had optimum improvement of gait and posture but with suboptimum control of rigidity and bradykinesia.

Cases with a more consistent control of all symptoms (P06, P09, and P10) had lesions involving the 3 fiber tracts comprising Raprl (Figure 2). In contrast, cases with transient improvement of symptoms had lesions outside Raprl fibers: 1 laterally on Zic and the other posteriorly, between Zic and medial lemniscus (Figure 3). In 2 cases, the lesion was performed inferior and medial to the intended target at the mesencephalic-pontine junction (P05 and P08), involving mainly cerebellar and GP-PPN components in the brain stem, had optimum control of tremor, posture, and gait (Table 3 and Figure 7).

DISCUSSION

Correlation of Fiber Lesioning With Changes in Severity of Symptoms

Despite our small sample of patients, Spearman correlations show that surgical disruption of connectivity of CCx is associated with improvement of symptoms of extremities contralateral to Raprl lesions, which is in line with previous reports[3-6] and with similar effects to DBS in this area.[7,8,10,12,34-38] Lesions of

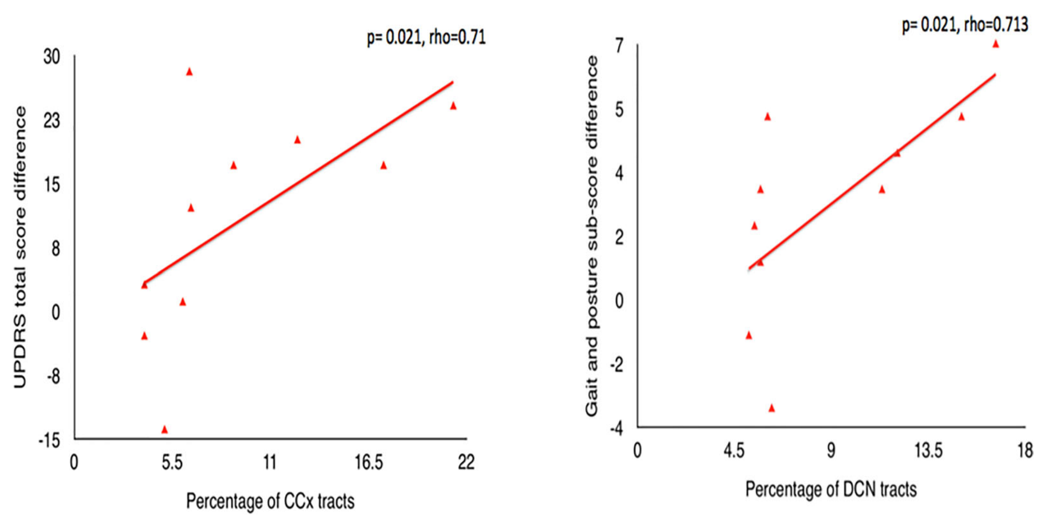

FIGURE 5. *Correlations between gait and posture and percentage of tracts within the surgical lesion of Raprl. Involvement of fibers connecting to the CCx and DCN, respectively, results in gait and posture improvement.*

fibers connecting contralateral DCNs are in turn associated with posture and gait improvements.

In contrast, we found a negative correlation between lesions in fibers connecting PFC pars opercularis and ventral middle frontal gyrus, Pu, and GP and improvement in posture and gait. It is worth noting that these symptoms are axial and therefore under the control of both hemispheres; hence, progression of PD in the nontreated hemisphere may jeopardize improvement of this symptom. Moreover, in the present series, gait and posture had improved at last follow-up in all but 1 patient.

In our cases, 0.8% involvement of fibers connecting Raprl with the middle frontal gyrus correlated with less improvement in posture and gait. In other studies, gait control mediated by PFC has been proposed, based on information derived from a morphometric MRI analysis of voxels of gray and white matter in PD patients with deterioration of executive functions and freezing gait. Atrophy of middle right frontal gyrus correlated with the severity of the dysfunction.[39] Decrease in connectivity studied through MRI and tract-based spatial statistics for frontal lobes showed a correlation with deterioration in executive functions in PFC.[40] Studies focusing on the anatomical location of PFC fibers connecting with Raprl might prevent negative outcomes in the future.

In our study, RF lesions were clearly delineated in their location and extension in postsurgical structural MRI, representing an advantage over DBS for determining the affected fiber tracts in the presurgical MRI. This series derives important information.

Our observations highlight that lesions in PSA effective at controlling PD symptoms were located on fiber tracts and not in nuclei (Figure 1). Zic has been proposed as a target to treat tremor of different etiologies[41,42] and Raprl and Zic are in close anatomical relation but may be differentiated by microelectrode recording.[11,12,43] The only case with a lesion in Zic had only partial control of tremor (50%), without improvement in other PD symptoms. In the 2 patients with transient improvement of symptoms, ending in poor results, lesions were outside Raprl, and transient improvement may be related to edema secondary to increased temperature during RF lesion (Figure 3). The practical implication is that for future targeting in PSA, DWI-MRI and tractography may better orient trajectories of electrodes for lesions or DBS.

On the other hand, lesions of fibers disrupting only a small part of the tract result in long-lasting improvement of symptoms. This was true not only for "positive symptoms," such as tremor and rigidity, but also for "negative symptoms" like bradykinesia, gait, and posture,[44] indicating that lesions modulate overactive circuits involved in the physiopathology of all motor symptoms in PD. Therefore, the volume of lesions may be reduced while still achieving adequate control of symptoms, decreasing the possibility of having undesired side effects.

Different Fiber Tracts Mediate Different Symptoms

Heterogenous improvement of symptoms in cases herein presented indicates that, even in the small volume of Raprl, lesions affected fibers mediating different symptoms. In fact, the stereotactic coordinates used for Raprl in the past[4-6] correspond to the lateral part of Raprl and induced improvement of tremor over other PD symptoms. When MRI became available, the target changed for the "x" coordinate to 4.5/10 because lesions induced better control of rigidity and gait.[7,8,11,12] In our series,

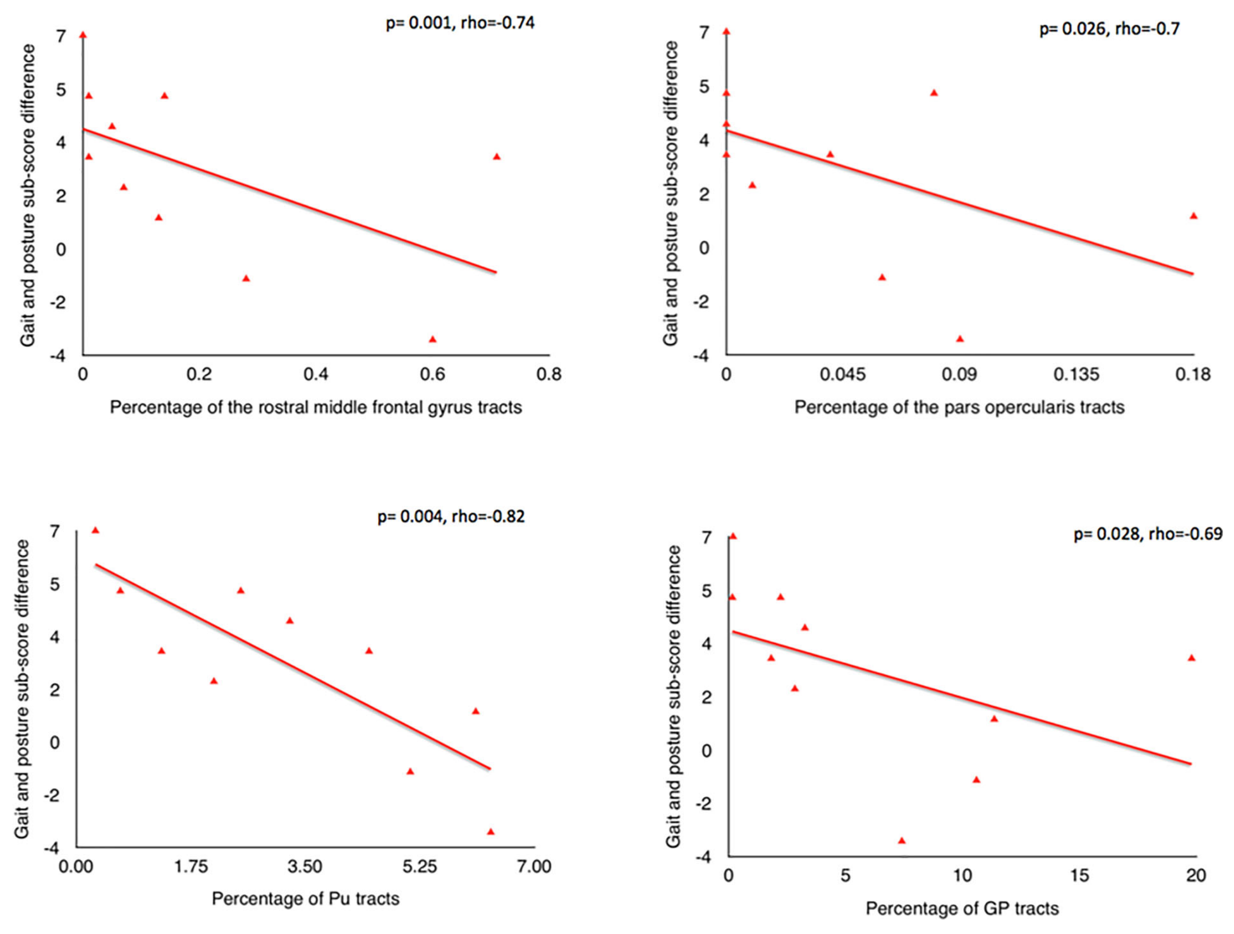

FIGURE 6. *Negative correlations between gait and posture UPDRS scores and percent of fiber tracts within the Raprl lesion that were associated with frontal middle gyrus and pars opercularis, Pu, and GP.*

TABLE 2. Symptom Improvements

Variable (UPDRS items)	Max possible score UPDRS-III	Basal mean (SD)	Final follow-up (SD)	% d	*P*
Tremor (Items 20-21)	12	7.90 (2.42)	1.09 (1.81)	−86	.001
Rigidity (Item 22)	8	4.54 (2.11)	1.90 (2.16)	−62	.015
Bradykinesia (Items 23-26 and 31)	20	7.81 (4.19)	3.81 (3.84)	−56	.046
Gait/Posture (Items 27-30)	16	5.27 (2.83)	1.90 (1.70)	−45	.001

Possible max score = maximal possible scores for unilateral tremor, rigidity, bradykinesia, posture, and gait in UPDRS-III. Basal mean = preoperative condition of patients for unilateral tremor and rigidity, and bradykinesia posture and gait. Mean value score for final UPDRS-III evaluation. Δ%d = percent decrease of symptom severity. Significance of changes for each symptom is indicated.

of 6 cases with optimum control of tremor, 2 had poor control of rigidity while 1 case with optimum control of rigidity had suboptimum control of tremor. In the case with the smallest lesion size, tremor was selectively improved while rigidity remained unchanged, indicating that there are different cerebellar thalamic fibers mediating these 2 symptoms. Recently, we reported a case with selective control of tremor that had an RF lesion placed in the base of the thalamus, involving the cerebellar-thalamic fibers

TABLE 3. Detailed UPDRS-III Pre-/Postsurgical Score for Each Patient in Right (R) and Left (L) Extremities

Patients	Operated side	T pre/post	R pre/post	B pre/post	G and P pre/post	Global UDRS pre/post	Lesion size (mm^3)
P01	Left	R6-L0/	R5-L1/	R8-L0/	4/3	47/44	46.65
		R3-L3	R 5-L2	R8-L5			
P02	Right	R4-L8/	R2-L4/	R4-L12/	9/5	60/70	46.25
		R4-L6	R2-L5	R3-L8			
P03	Right	R0-L14/	R0-L6/	R4-L14/	2/5	61/75	10.15
		R9-L0	R6-L5	R14-L11			
P04	Left	R8-L2/	R4-L1/	R11-L6/	9/5	50/53	30.42
		R0-L5	R4-L2	R4-L4			
P05	Left	R10-L0/	R8-L2/	R12-L4/	6/1	60/36	42.25
		R1-L0	R4-L1	R8-L4			
P06	Right	R0-L7/	R1-L3/	R2-L0/	3/1	39/11	25.1
		R0-L0	R1-L0	R1-L0			
P07	Left	R7-L0/	R4-L1/	R4-L2/	4/1	32/20	50.14
		R2-L0	R0-L0	R1-L2			
P08	Left	R8-L3/	R4-L1/	R8-L3/	6/1	40/23	68.1
		R2-L4	R1-L0	R4-L0			
P09	Left	R8-L3/	R8-L2/	R7-L3/	9/5	74/57	37.37
		R1-L6	R1-L4	R1-L9			
P10	Left	R5-L0/R0-L0	R1-L1/R0-L2	R5-L0/R2-L3	5/2	40/20	34.73

UPDRS items for tremor (T) 20 and 21, 22 for rigidity (R); 23 to 26 and 31 for bradykinesia (B); 27 to 30 for gait and posture (G and P). Pre-/postoperative changes for global UPDRS-III and volume of lesion size are indicated.

connecting with Vim leaving intact fibers ending in Vop, which probably controls rigidity.[45] This is in concordance with the fact that both DBS in Gpi connecting with Vop via the thalamic fasciculus[46,47] and DBS in Raprl connecting DCN with Vop, improve rigidity over tremor.

In previous reports, improvement in bradykinesia with Raprl lesions and DBS was not significant, probably because bradykinesia was incipient in the candidates for Raprl lesions[6] or DBS at that time.[7] However, when cases in stages Hoehn-Yahr IV-V were included, bradykinesia significantly improved by bilateral Raprl-DBS.[8] Probabilistic tractography of PSA revealed fibers connecting mesencephalic tegmentum (MES) with OFC, running medial and dorsal to STN, traversing Raprl in the uppermost segments toward MES.[9] OFC has been proposed as a potent inhibitor of emotional and motor behavior[48-49] and connecting fibers with the brain stem may mediate bradykinesia. Unilateral Raprl-DBS is also associated with bilateral glucose hypometabolism of OFC.[50] The location of this tract in Raprl, away from coordinates we have used for this target, is perhaps the reason that improvement of bradykinesia in this series was less reliable ($P < .046$) than for tremor ($P < .001$) and rigidity ($P < .015$).

Although our patients had only mild posture and gait disturbances, Raprl lesions significant improvement these symptoms (Table 2). In 2 patients (P05 and P08) where gait and posture improvement surpassed that of rigidity and bradykinesia, macro stimulation during operation did not induce the expected improvement at the intended target, so the exploration continued beyond the target to obtain adequate control of tremor at the place of lesioning. Postoperative MRI demonstrated that trajectories of the electrodes were medial to our intended target and the lesions located below the Ru.

Planning Based on Tractography Allows Targeting Fibers for Selective Improvement of Symptoms

Fiber tracts comprising Raprl have a point of maximal proximity where discrete lesions may improve all symptoms in a uniform manner, like in some of our cases (Figure 2 and Table 3). Extending away from this point, fiber tracts spread apart toward their anatomical connectivity. Therefore, it might be that surgical planning based on tractography allows targeting fibers for selective improvement of symptoms.

CONCLUSION

Lesion of fiber tracts (and not nuclei) in the PSA are responsible for PD symptom improvement. Different fiber tracts mediate different symptoms. Small lesions at the Raprl core, involving only part of the whole fiber tracts, resulted in over 2-yr improvement. Lesions (and DBS) directed at selected fiber tracts may result in selective improvement of symptoms tailored for each patient's needs.

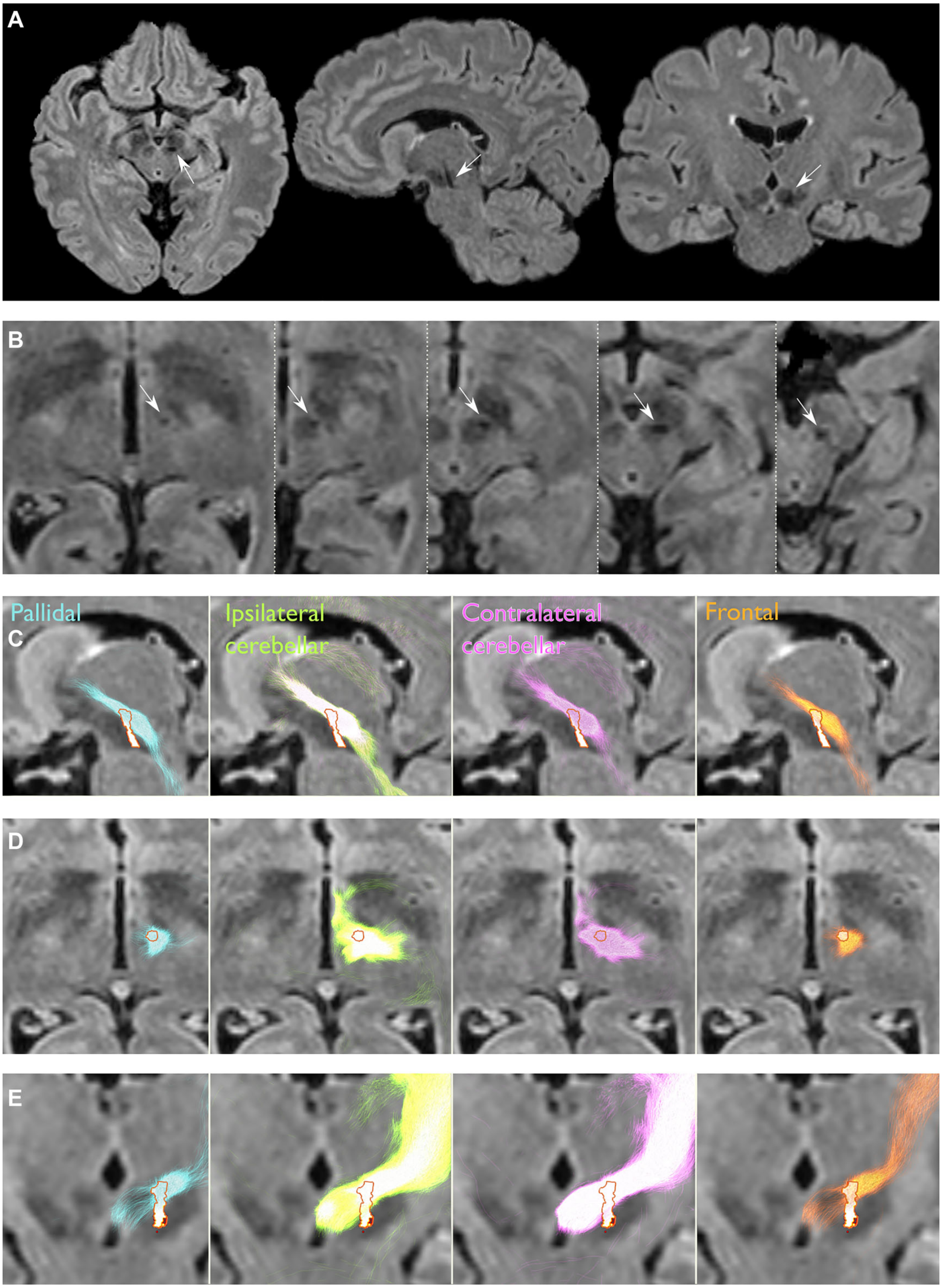

FIGURE 7. *RF lesion in P05 case intended for Raprl.* **A** *and* **B**, *postsurgical structural MRI axial view of the trajectory in PSA that traversed Ru and ended below the nucleus (arrows).* **C**, **D**, *and* **E**, *axial, coronal, and sagittal views showing an elongated lesion mainly affecting pallidal and cerebellar fibers.*

Disclosures

The authors have no personal, financial, or institutional interest in any of the drugs, materials, or devices described in this article. Dr García-Gomar received fellowship 275 789 from The National Council of Science and Technology, Mexico (Consejo Nacional de Ciencia y Tecnología, CONACYT), and support from Programa de Apoyo a los Estudios de Posgrado (PAEP).

REFERENCES

1. Spiegel EA, Wycis HT, Szekely EG, Baird HW 3rd, Adams J, Flanagan M. Campotomy. *Trans Am Neurol Assoc*. 1962;87:240-242.
2. Andy OJ, Jurko MF. Alteration in Parkinson tremor during electrode insertion. *Confin Neurol*. 1965;26(3):378-381.
3. Bertrand CHJ, Molina-Negro P, Martínez N. Optimum physiological target for the arrest of tremor. In *Third Symposium on Parkinson's Disease*. Living-Stone Pub. Edinburgh; 1969:251-259.
4. Velasco FC, Molina-Negro P, Bertrand C, Hardy J. Further definition of the subthalamic target for arrest of tremor. *J Neurosurg*. 1972;36(2):184-191.
5. Ito Z. Stimulation and destruction of the prelemniscal radiation or its adjacent area in various extrapyramidal disorders. *Confin Neurol*. 1975;37(1-3):41-48.
6. Velasco F, Velasco M. A reticulo-thalamic system mediating ptopioceptive attention and tremor in man. *Neurosurgery*. 1979;4(1):30-36.
7. Velasco F, Jimenez F, Perez ML, et al. Electrical stimulation of the prelemniscal radiation in the treatment of Parkinson's disease: an old target revised with new techniques. *Neurosurgery*. 2001;49(2):293-306; discussion 306-298.
8. Carrillo-Ruiz JD, Velasco F, Jimenez F, et al. Bilateral electrical stimulation of prelemniscal radiations in the treatment of advanced Parkinson's disease. *Neurosurgery*. 2008;62(2):347-357; discussion 357-349.
9. García-Gomar MG, Soto-Abraham J, Velasco-Campos F, Concha L. Anatomic characterization of prelemniscal radiations by probabilistic tractography: implications in Parkinson's disease. *Brain Struct Funct*. 2017;222(1):71-81.
10. Kitagawa M, Murata J, Uesugi H, et al. Two year follow-up of chronic stimulation of posterior subthalamic white matter for tremor dominant Parkinson's disease. *Neurosurgery.* 2005;56(2):281-289.
11. Castro G, Carrillo-Ruiz JD, Salcido V, et al. Optimizing prelemniscal radiations as a target for motor symptoms in Parkinson's disease treatment. *Stereotact Funct Neurosurg*. 2015;93(4):282-291.
12. Velasco F, Carrillo-Ruiz JD, Salcido V, Castro G, Soto J, Velasco AL. Unilateral stimulation of prelemniscal radiations for the treatment of acral symptoms of Parkinson's disease: long-term results. *Neuromodulation*. 2016;19(4):357-364.
13. Higuchi Y, Matsuda S, Serizawa T. Gamma knife radiosurgery in movement disorders: indications and limitations. *Mov Disord*. 2017;32(1):28-35.
14. Takeda N, Horisawa S, Taira T, Kawamata T. Radiofrequency lesioning through deep brain stimulation electrodes in patients with generalized dystonia. *World Neurosurg*. 2018;115:220-224.
15. Tsolaki E, Downes A, Speier W, Elias WJ, Pouratian N. The potential value of probabilistic tractography-based for MR-guided focused ultrasound thalamotomy for essential tremor. *Neuroimage Clin*. 2018;17:1019-1027.
16. Jourdain VA, Schechtmann G. Health economics and surgical treatment for Parkinson's disease in a world perspective: results from an international survey. *Stereotact Funct Neurosurg*. 2014;92(2):71-79.
17. Tournier JD, Calamante F, Connelly A. Robust determination of the fibre orientation distribution in diffusion MRI: non-negativity constrained super-resolved spherical deconvolution. *Neuroimage*. 2007;35(4):1459-1472.
18. Sammartino F, Yeh FC, Krishna V. Longitudinal analysis of structural changes following unilateral focused ultrasound thalamotomy. *Neuroimage Clin*. 2019;22:101754.
19. Desikan RS, Segonne F, Fischl B, et al. An automated labeling system for subdividing the human cerebral cortex on MRI scans into gyral based regions of interest. *Neuroimage*. 2006;31(3):968-980.
20. Manjon JV, Coupe P. volBrain: an online MRI brain volumetry system. *Front Neuroinform*. 2016;10:30.
21. Calamante F, Tournier JD, Heidemann RM, Anwander A, Jackson GD, Connelly A. Track density imaging (TDI): validation of super resolution property. *Neuroimage*. 2011;56(3):1259-1266.
22. Calamante F, Tournier JD, Smith RE, Connelly A. A generalised framework for super-resolution track-weighted imaging. *Neuroimage*. 2012;59(3): 2494-2503.
23. Wu D, Reisinger D, Xu J, et al.. Localized diffusion magnetic resonance microimaging of the live mouse brain. *Neuroimage*. 2014;91:12-20.
24. Hoch MJ, Chung S, Ben-Eliezer N, Bruno MT, Fatterpekar GM, Shepherd TM. New clinically feasible 3T MRI protocol to discriminate internal brain stem anatomy. *AJNR Am J Neuroradiol*. 2016;37(6):1058-1065.
25. Schaltenbrand G, Wahren W. *Atlas for Stereotaxy of the Human Brain*. Chicago-London: Georg Thieme Publisher; 1977.
26. García-Gomar MG, Concha L, Alcauter S, et al. Probabilistic tractography of the posterior subthalamic area in Parkinson's disease patients. *J Biomed Sci Eng*. 2013;6(3):381-390.
27. Smith RE, Tournier JD, Calamante F, Connelly A. Anatomically-constrained tractography: improved diffusion MRI streamlines tractography through effective use of anatomical information. *Neuroimage*. 2012;62(3): 1924-1938.
28. Smith RE, Tournier JD, Calamante F, Connelly A. SIFT: spherical-deconvolution informed filtering of tractograms. *Neuroimage*. 2013;67:298-312.
29. Smith RE, Tournier JD, Calamante F, Connelly A. SIFT2: enabling dense quantitative assessment of brain white matter connectivity using streamlines tractography. *Neuroimage*. 2015;119:338-351.
30. Ewert S, Plettig P, Li N, et al. Toward defining deep brain stimulation targets in MNI space: a subcortical atlas based on multimodal MRI, histology and structural connectivity. *Neuroimage*. 2018;170:271-282.
31. Fonov V, Evans AC, Botteron K, Almli CR, McKinstry RC, Collins DL. Unbiased average age-appropriate atlases for pediatric studies. *Neuroimage*. 2011;54(1):313-327.
32. Keuken MC, Bazin PL, Schafer A, Neumann J, Turner R, Forstmann BU. Ultra-high 7T MRI of structural age-related changes of the subthalamic nucleus. *J Neurosci*. 2013;33(11):4896-4900.
33. Massey LA, Miranda MA, Zrinzo L, et al. High resolution anatomy of the subthalamic nucleus: imaging at 9.4 T with histological validation. *Neuroimage.* 2012;59(3):2035-2044.
34. Forstmann BU, Keuken MC, Jahfari S, et al. Cortico-subthalamic white matter tract; strength predicts interindividual efficacy in stopping a motor response. *Neuroimage*. 2012;60(1):370-375.
35. Hamel W, Herzog J, Kopper F, et al. Deep brain stimulation in the subthalamic area is more effective than nucleus ventralis intermedius stimulation for bilateral intention tremor. *Acta Neurochir (Wien)*. 2007;149(8):749-758; discussion 758.
36. Coenen VA, Allert N, Madler B. A role of diffusion tensor imaging fiber tracking in deep brain stimulation surgery: DBS of the dentato-rubro-thalamic tract (DRT) for the treatment of therapy-refractory tremor. *Acta Neurochir (Wien)*. 2011;153(8):1579-1585; discussion 1585.
37. Coenen VA, Allert N, Paus S, Kronenburger M, Urbach H, Madler B. Modulation of the cerebello-thalamo-cortical network in thalamic deep brain stimulation for tremor: a diffusion tensor imaging study. *Neurosurgery*. 2014;75(6):657-669; discussion 669-670.
38. Sweet JA, Walter BL, Gunalan K, Chaturvedi A, McIntyre CC, Miller JP. Fiber tractography of the axonal pathways linking the basal ganglia and cerebellum in Parkinson disease: implications for targeting in deep brain stimulation. *J Neurosurg*. 2014;120(4):988-996.
39. Brugger F, Abela E, Hahgele-Link S, Bohlhalter S, Galovic M, Kagi G. Do executive dysfunction and freezing gait in Parkinson's disease share the same neuroanatimical correlates? *J Neurol Sci*. 2015;356(1-2): 184-187.
40. Dimberger G, Jahanshahi M. Executive dysfunction in Parkinson's disease: a review. *J Neuropsychol*. 2013;7(2):193-224.
41. Plaha P, Ben-Shlomo Y, Patel NK, Gill SS. Stimulation of the caudal zona incerta is superior to stimulation of the subthalamic nucleus in improving contralateral Parkinsonism. *Brain*. 2006;129(Pt 7):1732-1747.
42. Fytagoridis A, Astrom M, Samuelsson J, Blomstedt P. Deep brain stimulation of the caudal zona incerta: tremor control in relation to the location of stimulation fields. *Stereotact Funct Neurosurg*. 2016;94(6):363-370.
43. Merello M, Tenca E, Cerquetti D. Neuronal activity of the zona incerta in Parkinson's disease patients. *Mov Disord*. 2006;21(7):937-943.

44. Martin-Purdon J HL, Finlayson MH. The negative symptoms of basal ganglia disease. *Lancet*. 1962;2(7246):62-66.
45. Velasco F, Esqueda-Liquidano M, Velasco AL, Garcia-Gomar MG. Prelemniscal lesion for selective improvement of Parkinson disease tremor. *Stereotact Funct Neurosurg*. 2018;96(1):54-59.
46. Gallay MN, Jeanmonod D, Liu J, Morel A. Human pallidothalamic and cerebellothalamic tracts: anatomical basis for functional stereotactic neurosurgery. *Brain Struct Funct*. 2008;212(6):443-463.
47. Fukuda M, Mentis MJ, Ma Y, et al. Networks mediating the clinical effects of pallidal brain stimulation for Parkinson's disease: a PET study of resting-state glucose metabolism. *Brain*. 2001;124(Pt 8):1601-1609.
48. Velasco F, Velasco M, Jimenez F, Velasco AL, Salin-Pascual R. Neurobiological background for performing surgical intervention in the inferior thalamic peduncle for treatment of major depression disorders. *Neurosurgery*. 2005;57(3):439-448; discussion 439-448.
49. Coenen VA, Schumacher LV, Kaller C, et al. The anatomy of the human medial forebrain bundle: ventral tegmental area connections to reward-associated subcortical and frontal lobe regions. *Neuroimage Clin*. 2018;18:770-783.
50. Velasco F, Llanos S, Avila-Rodriguez MA, et al. Metabolic changes induced by electrical stimulation of prelemniscal radiations for the treatment of Parkinson disease. *Stereotact Funct Neurosurg*. 2015;93(5):333-341.

Acknowledgments

The authors are grateful to the patients and their families for their cooperation. Images were acquired at the National Laboratory for Magnetic Resonance Imaging (UNAM, CONACYT, CIMAT, UAQ). We thank Erick Pasaye, Juan Ortiz, Leopoldo González, and the personnel of the Magnetic Resonance Unit for technical assistance, and Jessica González Norris for proofreading and editing.

COMMENT

The authors elegantly describe their valuable experience in 10 patients with Parkinson disease treated with targeted ablation of preliminiscal fiber tracts. While the number of patients is small, this study is unique and valuable on multiple fronts. First, in an era where deep brain stimulation dominates the literature for surgical therapies for Parkinson disease, it is important to be reminded of the value of targeted lesions. Second, while the goals in stereotactic surgery are often consistency, precision, and accuracy, this study reminds us that measured variability is indeed valuable - to target specific symptomatology based on patient-specific needs as well as for better understanding the efficacy of our treatment in a symptom- and tract-specific manner. Finally, the authors' work highlights the value to studying brain connectivity in understanding the functional neurosurgical interventions, be it stimulation or ablation. However, as a clinical and academic community, we must remain cognizant of the limitations of imaging and the interpretation of these results, particularly when evaluating multiple tracts in small areas such as the prelimnisal fiber tracts. Still, while these may not be perfectly accurate representations of underlying anatomy, there is still very likely value in the reported results as symptom-specific imaging biomarkers. Prospective mapping and evaluation would be extremely valuable moving forward.

Nader Pouratian
Los Angeles, California